Fractionation of Freshwater Colloids and Particles by SPLITT: Analysis by Electron Microscopy and 3D Excitation−Emission Matrix Fluorescence

J. R. Lead,* A. De Momi, G. Goula, and A. Baker

School of Geography, Earth and Environmental Sciences, University of Birmingham, Birmingham, B15 2TT., U.K.

This paper reports the first application of a combined approach utilizing split-flow thin-cell (SPLITT) separation to size fractionate natural aquatic colloids and particles collected from freshwater samples. No sample preconcentration was performed although some samples were investigated after alteration of the ambient pH. The unfractionated and fractionated samples were analyzed by scanning electron microscopy (SEM), environmental SEM, and 3D excitation emission matrix fluorescence. Qualitative and quantitative results by microscopy indicated that SPLITT produces well-resolved fractionations at appropriate sizes but with some perturbation of the sample. In addition, tryptophan-like fluorescence was shown to be caused by different organic moieties compared with humic-like and fulvic-like fluorescence. Tryptophan-like fluorescence intensity is found mainly in the particulate material but is not pH dependent, while humic- and fulvic-like fluorescence intensities are dependent on pH but not on size. Fulvic-like fluorescence intensity normalized to absorbance, related to fluorescence efficiency and molar mass, varies with size.

Natural aquatic colloids are defined as solid-phase material with one dimension within the range 1 nm−1 μm in natural waters, while particles are greater than 1 μm.[1,2] As interactions of pathogens and chemical pollutants are dominated by these phases, they largely determine the biological impact, fate, and behavior of the contaminants. It is therefore essential to have suitable methodologies to separate and analyze aquatic colloids and particles. Conceptual or actual separation of suspended material into colloids and particles is of particular use due to their different behavior in waters. For instance, colloids are dominated by aggregation processes and particles by sedimentation processes[3] producing geochemical fractionation in the associated contaminants. Recent developments in both SPLITT separation[4−6] and fluorescence[7] have made these techniques potentially suitable for the provision of high-quality information on colloids and particles.

SPLITT has been used occasionally, since the first reports on monodisperse laboratory standards,[8,9] as an option to traditional membrane filtration. As separations are made at a continuously renewed liquid boundary layer, the artifacts inherent in filtration (the standard method) due to solute−membrane interactions are removed.[1] Nevertheless, the methodology has not been fully tested for use in natural waters. The method has been used to fractionate both sediment[5,10] and natural water particles[11,12] including diatoms[4] and has been coupled with various analytical techniques to measure organic carbon, major and trace elements,[11,13] and organic contaminants.[10] Although the separation is complex and based on a number of factors including buoyant mass,[6] values are usually reported as size. Indeed, partial verification of accurate size fractionation has been performed in natural waters by electron microscopy[11,12] and in marine sediments.[5,10] However, full and quantitative verification of the SPLITT fractionation has not been reported in the literature. In particular, here we have investigated the original and fractionated waters and used the minimally perturbing method of environmental scanning electron microscopy (ESEM), where colloids and particles can be imaged and quantified in their hydrated state down to a resolution of ~30 nm for natural aquatic material.[14]

Fluorescence spectroscopy is widely used in medical optics and biotechnology, as fluorescence is the end detection point of

* Corresponding author. E-mail: j.r.lead@bham.ac.uk. Fax: (+44) 121 414 5528.

(1) Lead, J. R.; Davison, W.; Hamilton-Taylor, J.; Buffle, J. *Aquat. Geochem.* **1997**, *3*, 213−232.
(2) Buffle, J., van Leeuwen, H. P., Eds. *Environmental particles*; Lewis Publishers: Boca Raton, FL. 1992.
(3) Buffle, J.; Leppard, G. G. *Environ. Sci. Technol.* **1995**, *29*, 2169−2175.
(4) Rings, A.; Lucke, A.; Schleser, G. h. *Limnol. Oceanogr.: Methods* **2004**, *2*, 25−34.
(5) Moon, M. H.; Kim, H.-J.; Kwon, S.-Y.; Lee, S.-J.; Chang, Y. S.; Lim, H. *Anal. Chem.* **2004**, *76*, 3236−3243.
(6) Coppola, L.; Gustafsson, O.; Andersson, P.; Axelsson, P. *Water Res.* **2005**, *39*, 1935−1945.
(7) Baker, A.; Inverarity, R. *Hydrol. Processes* **2004**, *18*, 2927−2945.
(8) Fuh, C. B.; Myers, M. N.; Giddings, J. C. *Anal. Chem.* **1992**, *64*, 3125−3132.
(9) Springston, S. R.; Myers, M. N.; Giddings, J. C. *Anal. Chem.* **1987**, *59*, 344−350.
(10) Moon, M. H.; Kim, H.-J.; Jung, Y.-O.; Lee, S.-J.; Chang, Y.-S. *J. Sep. Sci.* **2005**, *28*, 373−379.
(11) Blo, G.; Contado, C.; Grandi, D.; Fagioli, F.; Dondi, F. *Anal. Chim. Acta* **2002**, *470*, 253−262.
(12) Contado, C.; Dondi, F.; Beckett, R.; Giddings, J. C. *Anal. Chim. Acta* **1997**, *345*, 99−110.
(13) Kiem, R.; Knicker, H.; Kogel-Knabner, I. *Org. Geochem.* **2002**, *33*, 1683−1697.
(14) Redwood, P. S.; Lead, J. R.; Harrison, R. M.; Stoll, S. *Environ. Sci. Technol.* **2005**, *39*, 1962−1966.

10.1021/ac0521347 CCC: $33.50
Published on Web 00/00/0000

a majority of biological measurement.[15] This driver has led to substantive technological improvements that can be used by environmental scientists. For instance, rapid wavelength scan speeds, analysis of the 200−300-nm range where much environmentally relevant intrinsic fluorescence occurs,[7] and measurement over both excitation and emission wavelengths over the whole 190−800-nm range (excitation−emission matrixes or EEMs) can now be performed with relative ease. Four fluorophores in natural organic matter have been commonly identified: (1) tyrosine-like fluorescence (also known as peak B,[16] or γ[17]) excites at 220−235 nm and emits at 290−310 nm; (2) tryptophan-like fluorescence (also peak T or δ) at 220−240-nm excitation and 340−360-nm emission; (3) humic-like fluorescence at 300−350-nm excitation and 400−450-nm emission (termed peak C, α, or fulvic-like); (4) humic-like fluorescence at 220−240-nm excitation and 400−450-nm emission (peak A, α′ or humic-like). It has been observed that the analysis of smaller molar mass fractions of organic matter results in higher fluorescence emission intensities and shorter emission wavelengths of peaks C and A, in comparison to larger mass fractions.[18] Senesi and colleagues[19] related this to the greater proximity of chromophores in higher molecular weight DOM and an increased probability of internal quenching occurring such as collisional deactivation. Additionally, increased rigidity in molecules was related to increases in fluorescence intensity, due to a reduction in internal conversions.[19] Finally, the fluorescence intensity per centimeter absorbance or milligram of C provides a measure of fluorescence efficiency, which could also be related to molar mass or aquatic colloid function.[20] Nevertheless, little is understood about the relationship between size and fluorescence.

This paper reports the first coupling of SPLITT to scanning electron microscopy (SEM), ESEM, and 3D excitation−emission matrix (EEM) fluorescence for the fractionation and analysis of natural aquatic colloids and particles.

METHODOLOGY

Sample Collection and Processing. Samples were taken from the Vale Lake, West Midlands, U.K., on three occasions: 20 August 2004, 18 November 2004, and 3 February 2005. Samples were taken from the lake side just below the water surface. All collection bottles were polythene, rinsed with dilute nitric acid, pure water ($R = 18.2$ mΩ cm), and the lake water. Washings were discarded. Samples were taken with great care using procedures to minimize any changes in natural aquatic colloids and particles.[21] Temperature and pH were measured at the time of sampling. Samples were returned to the laboratory immediately, and fractionation and analysis were performed immediately and finished within 48 h. Where necessary, water samples were stored at 4 °C in the dark prior to fractionation and analysis. Unusually for SPLITT analysis of environmental samples, no preconcentration of the samples was required due the postconcentration (after fractionation) in sample preparation and the very high sensitivity of the analysis. For some analysis, sample pH was varied between 5.5 and 9.5 by the addition of dilute nitric acid or sodium hydroxide, without the use of buffers. Samples were shaken for ∼4 h until a constant pH value was reached. Fractionation occurred over a few minutes, which helped to minimize any changes in pH, and pH was monitored both before and after SPLITT fractionation

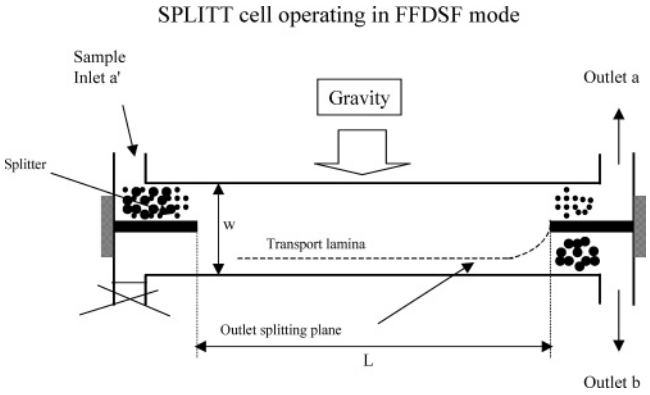

Figure 1. Schematic diagram of the SPLITT cell operation.

SPLITT Fractionation. The theory of SPLITT fractionation is well known,[8] and we present a brief summary here. SPLITT is an extension of the field flow fractionation techniques,[22] which permits a binary separation of solid-phase material in a manner analogous to filtration. Separation is performed by the action of gravitational force acting perpendicularly to a laminar flow of a thin channel and the separation driven by a force acting perpendicularly to the sample flow. Thus, the primary mechanism of fractionation is settling velocity, although other parameters may be important, such as diffusion coefficient for small material. The separation mechanisms are only poorly known in their application to natural aquatic colloids and particles. In this work, only one sample inlet was used (the so-called full feed depletion (FFD) mode[11]) and a hypothetical outer splitting plane (OSP) is produced as shown in Figure 1. Previous work[11] has shown this mode to provide more rapid separations and to reduce dilution compared with the conventional (two-inlet) mode. The solid-phase components assume an equilibrium position in the channel flow, and different flow planes are mechanically separated at the channel terminus by baffles set in the channel. Solid-phase material with sufficient mass settle through the OSP and are eluted through outlet b, while those sufficiently buoyant do not penetrate the OSP and are eluted through channel a. In this work, gravitational force was used, limiting the lower cutoff limit to 1 μm, using an assumed particle density of 2.5 g mL^{-1}, and shapes were calculated after analysis. This cutoff was used here and has particular utility for the separation of environmental colloids and particles.

A brief description of SPLITT theory is given below. The general expression for the volumetric flow rate passing

(15) Lacowicz, J. R. *Principles of Fluorescence Spectroscopy*, 2nd ed.; Kluwer Academic: New York, 1999.
(16) Coble, P. G. *Mar. Chem.* **1996**, *51*, 325−346.
(17) Parlanti, E. *Org. Geochem.* **2000**, *31*, 1765−1781.
(18) Miano, T. M.; Alberts, J. J. In *Understanding Humic Substances: Advanced Methods, Properties and* Applications; Ghabbour, E. A., Davies, G., Eds.; Royal Society of Cambridge: Cambridge, UK, 1999.
(19) Senesi, N.; Miano, T. M.; Provenzano, M. R.; Brunetti, G. *Soil Sci.* **1991**, *152*, 259−271S.
(20) Thacker, A.; Tipping, E.; Baker, A.; Gondar, D. *Water Research*; Pergamon: New York, in press.
(21) Muirhead, D.; Lead, J. R. *Hydrobiologia* **2003**, *454*, 65−69.
(22) Beckett, R.; Hart, B. T. In *Environmental Particles*; Bufle, J., Leeuwen, H. P. v., Eds.; Lewis Press: New York, 1993; Vol. 2, pp 165−205.

along the transport region is

$$\dot{V}(t) = \dot{V}(a) - \dot{V}(a') = \dot{V}(b') - \dot{V}(b) \quad (1)$$

that for the FFDSF mode it becomes (only one inlet is used)

$$\dot{V}(t) = \dot{V}(a') - \dot{V}(b) \quad (2)$$

The volumetric flow rate can be also expressed by

$$\dot{V}(t) = bLU \quad (3)$$

where b is the cell breadth, L is the length, and U is the velocity of sedimentation. This equation can be rewritten as

$$\Delta\dot{V} = \frac{bLG(\rho_p - \rho)d^2}{18\eta} \quad (4)$$

where G is the gravity acceleration, ρ_p is the density of the particles, ρ is the carrier density, d is the diameter of the particles, and η is the viscosity of the carrier. The condition for which a particle exits from the outlet b is given by

$$\Delta\dot{V} \rangle \Delta\dot{V}(t) \quad (5)$$

Thus, particle diameter can be calculated for samples where other properties are known. In the case of natural colloids and particles, density can vary from analogous 1−5 g mL^{-1}, depending on the component being considered. We have chosen an overall density of 2.5 g mL^{-1}, as an average of these components and as a representative of mineral phases such as silica, which is a major component of many waters. It should be noted that, in FFDSF mode, the *a* fraction is expected to be free from large particles, while the *b* fraction is the natural water enriched in large particles (i.e., will still contain small colloids).

The SPLITT cell apparatus used was SF 1000HC (Postnova). Channel dimensions were 20 cm in length, 4 cm in width, and 964 μm in thickness, and sample was delivered to the SPLITT via a peristaltic pump. Flow conditions were adjusted to provide nominal cutoff diameters of 1 μm, using flow rates of 1 mL min^{-1} in the a′ (inlet), 0.66 mL min^{-1} in the a outlet (<1 μm), and 0.34 mL min^{-1} in the b outlet (>1 μm).

Electron Microscopy. Both SEM and ESEM were used to image the lake water and the SPLITT fractions (with nominal fractionations at 1 μm) and subsequently to derive particle size distributions (PSDs). A JEOL JSM-6060 LV was used to obtain morphological information on colloids and particles dried at ultrahigh vacuum. Droplets of sample were placed on a clean stub, air-dried, and coated with platinum with an Emscope SC500 sputter coater. The SEM acceleration was 15 kV. Lateral dimensions of ~400 particles were estimated for the PSDs. ESEM was used to provide information on colloids and particles in their fully hydrated state.[14,23] A single droplet of sample was placed onto a clean glass surface, which was fixed to ESEM stainless steel support stubs using graphite paint for reducing charge effects around the sample and then positioned on the water-cooled Peltier stage. Four drops of ultrapure water were placed on the cooling stage around the sample to control the sample humidity and minimize dehydration that may occur during evacuation of the air from the sample chamber.[24] These droplets were not imaged. Imaging was performed by an Philips XL30 ESEM in wet mode with an acceleration voltage of 10 kV and a pressure of ~5.4 Torr, using water as the vapor phase and a temperature of 2 °C, resulting in relative humidities of ~100% for all samples. No bulk liquid water was present which would interfere with imaging, but colloids and particles maintained substantial hydration water, helping to maintain the integrity of their easily perturbed structure. Lateral dimensions of ~400 particles were counted to generate PSDs. The advantages of using both SEM and ESEM for natural aquatic particles have been previously discussed by the authors.[25]

Shape factors were calculated form the equation, SF = 4π(area/perimeter^2); $0 \le SF \le 1$), where a value of 1 was a sphere and values lower than 1 were increasingly less spherical and regular. Calculations were performed with the Gatan Inc. Digital Micrograph program version 3.4.4., and in all cases, several thousand individual particles were analyzed.

Fluorescence Analysis. Samples were collected in the field using cleaned glass or polypropylene sample bottles. Samples were refrigerated and analyzed within 48 h using a benchtop Varian Cary Eclipse luminescence spectrophotometer using published methods.[26] Fluorescence was excited from 200 to 370 nm and emission detected from 280 to 500 nm with slits set to 5 nm and a scan speed of 9600 nm/min. Calibration samples were regularly taken using distilled water and measuring the Raman intensity at 348-nm excitation wavelength: results were adjusted to a value to 20 intensity units.

RESULTS AND DISCUSSION

Sample Integrity and Accuracy of Data. For natural aquatic colloids, a number of authors[27−30] have recently discussed the absolute importance of using both nonperturbing sample handling, fractionation, and analysis methods and bringing several techniques to bear on the same sample. This approach ensures sample integrity and the accuracy of data and has been followed in this work. In addition, the wide range of data collected allows the determination of a realistic picture to be built up of the properties of these heterogeneous and polydisperse materials. Uniquely, to our knowledge, the water samples were not deliberately modified, e.g., by preconcentration, prior to fractionation and rigorous steps were taken to ensure that the samples were minimally perturbed by suitable sampling, handling, and storage strategies. The results therefore represent the in situ nature of the colloids and particles in an accurate manner, given the uncertainties inherent in the sampling step itself. In addition and uniquely, the sizing was fully quantified and validated by different types of electron microscopy

(23) Donald, A. M.; He, C. B. *Colloids Surf., A* **2000**, *174*, 37−53.
(24) Doucet, F. J.; Maguire, L.; Lead, J. R. *Anal. Chim. Acta* **2004**, *522*, 59−71.
(25) Doucet, F. J.; lead, J. R.; Maguire, L.; Achterberg, E.; Millward, G. *J. Environ. Monit.* **2005**, *7*, 115−121.
(26) Baker, A. *Environ. Sci. Technol.* **2001**, *35*, 948−953.
(27) Lead, J. R.; Balnois, E.; Hosse, M.; Menghetti, R.; Wilkinson, K. J. *Environ. Int.* **1999**, *25*, 245−258.
(28) Lead., J. R.; Wilkinson, K. J.; Balnois, E.; Cutak, B.; Larive, C.; Assemi, S.; Beckett, R. *Environ. Sci. Technol.* **2000**, *34*, 3508−3513.
(29) Liss, S. N.; Droppo, I. G.; Flanagan, S. T.; Leppard, G. G. *Environ. Sci. Technol.* **1996**, *30*, 680−686.
(30) Wilkinson, K. J.; Balnois, E.; Leppard, G. G.; Buffle, J. *Can. J. Fish. Aquat. Sci.* **1999**, *155*, 287−310.

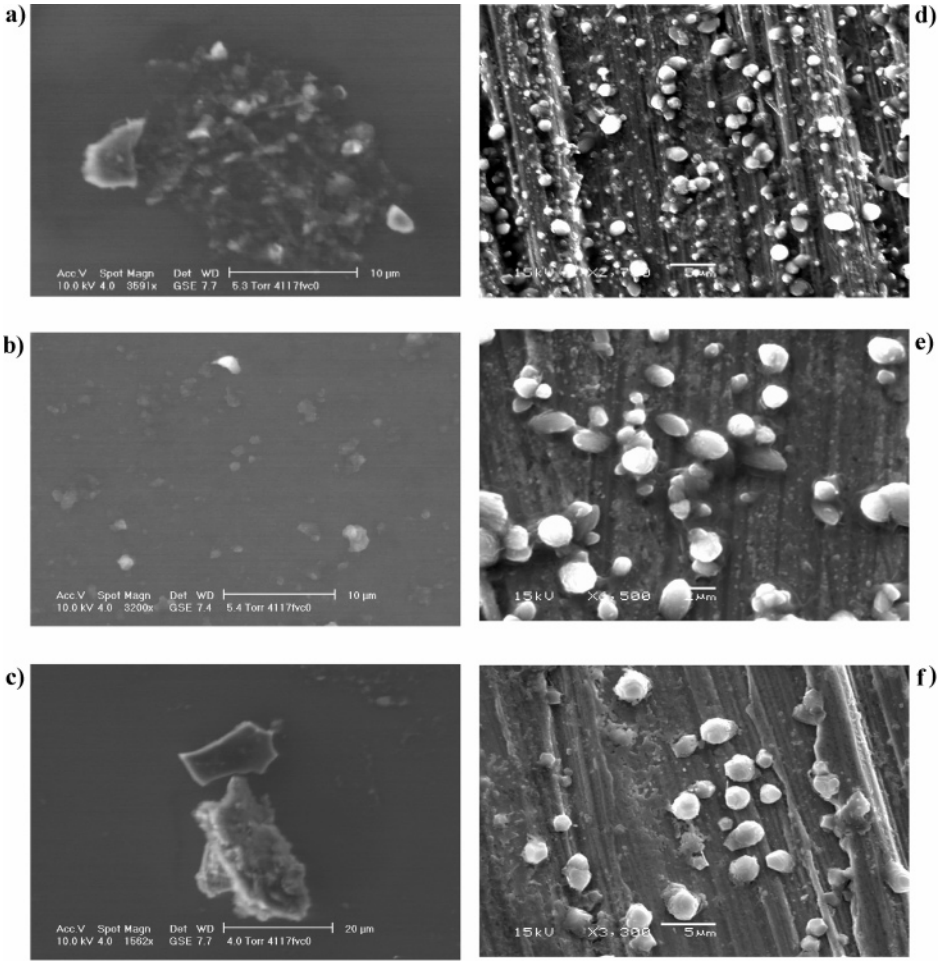

Figure 2. Selected ESEM images of unperturbed and size-fractionated lake water, (a) lake water, (b) <1-μm fraction, and (c) >1-μm fraction, and SEM images of unperturbed and size-fractionated lake water, (d) lake water, (e) <1-μm fraction, and (f) >1-μm fraction.

on the unfractionated sample and the fractionated eluent from the SPLITT system. Previous work has used SEM analysis alone to produce size distributions on the SPLITT eluent fractions[5,10] with consequent uncertainty of the role of sample drying and without knowledge of the original size distributions. Other literature data have qualitatively tested the accuracy of SPLITT[11,12] or simply assumed that SPLITT separates these complex materials according to theory, based on compact spheres, a problematic assumption for natural aquatic colloids and particles. Previously, the authors have combined SEM and ESEM[25] and found benefits from combining the higher resolution of the SEM with the less perturbing ESEM. In addition, fluorescence analysis has provided information about the distribution of both humic-type material and tryptophan-type material, as well as support for the accuracy of the sizing as discussed later.

Accuracy of SPLITT Fractionation. Representative SEM and ESEM images are shown in Figure 2. These figures are comparable with previous images of natural aquatic colloids and particles from SEM and ESEM.[25] It is clear that, whereas the SEM produces roughly spherical individual particles, sometimes on top of an aggregated surface layer, the ESEM produces more complex conformations and geometries, often as small aggregates or in a loose association with each other. This is indicative of the complex and fragile nature of the colloids and particles and the relatively perturbing nature of SEM. However, the conformations derived from ESEM present a difficulty in data interpretation as a particle size distribution, where discrete spheres are used. Nevertheless, qualitatively, the conformations are very roughly spherical and thus amenable to quantification by PSDs. By selection of a random sample of colloids and particles and use of a standardized procedure for assessing the size of slightly nonspherical particles, the PSD distributions appear to be consistent and comparable. Fibrillar and other nonspherical material often seen by transmission electron and atomic force microscopy[30] was not observed here, possibly because of the nature of the sample or, more likely, due to the different analytical methods.

Figures 3 and 4 show the PSDs from the ESEM and SEM images, respectively. In the original samples, particles were roughly evenly distributed between the different size fractions (~45% in the >1-μm fraction and ~55% in the <1-μm fraction, with slight differences observed between ESEM and SEM). Excellent separations are produced by SPLITT separations of 1 μm, indicating that the fractionation is working effectively. In particular, the *a* fraction for both SEM and ESEM (<1 μm) and the *b* fraction (>1 μm) by ESEM give greater than 90% of solid-phase material in the expected size range, indicating the essentially quantitative removal of large material from this fraction (Figure 1a, b, d). The *b* fraction from SEM shows a fractionation that is almost equally as good, with ~75−85% of the particles in the expected size range, indicating a slight contamination of this fraction by submicrometer-

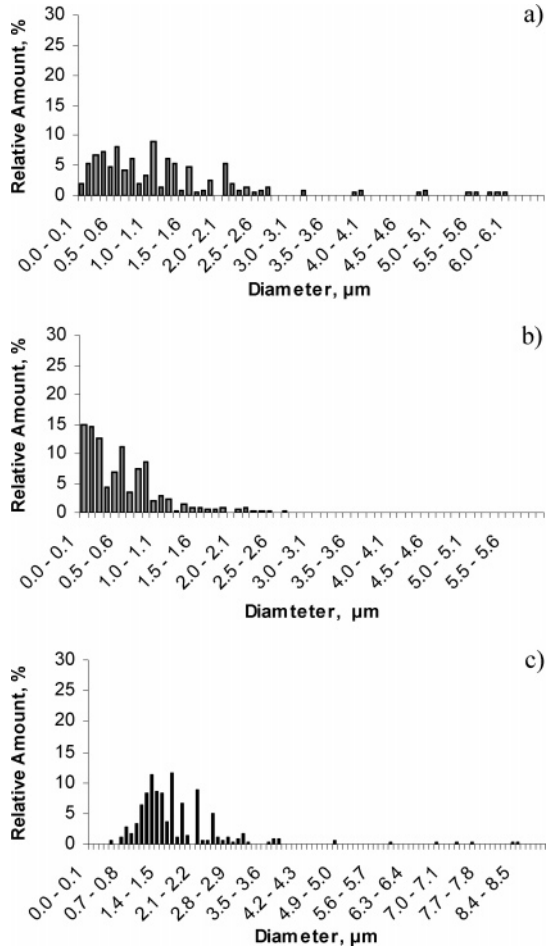

Figure 3. PSDs derived from ESEM data.

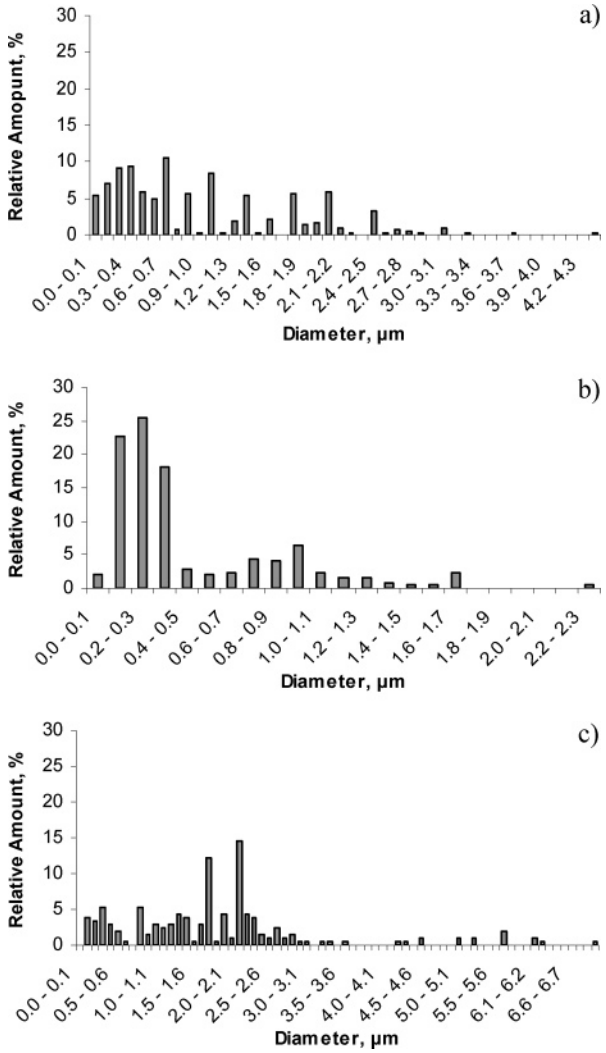

Figure 4. PSDs derived from SEM data.

sized colloids. The slightly reduced efficiencies are due to the fact that, in FFSDF mode, no separation of small material from the *b* fraction is effected by the SPLITT. The changes between the bulk sample and the *b* fraction are due only to enrichment by large particles. Nevertheless, the overall separation is highly effective, although somewhat variable between runs. Therefore, validation of the fractionation by microscopy or another technique is always required before and during routine use of SPLITT for quality assurance purposes. Any data collected without such confirmation must be subject to considerable uncertainties.

Further information on the particle morphologies was gained from analysis of shape factors between fractions and in relation to size. For spherical samples, a shape factor of 1 is expected. Values of ~0.37 ± 0.19 ($n = 1829$) in the bulk water were obtained, compared with 0.46 ± 0.18 ($n = 5594$) in the *a* fraction (<1 μm) and 0.44 ± 0.12 ($n = 7639$) in the *b* fraction (>1 μm). The mean shape factor of the bulk water is significantly lower than the SPLITT fractions ($p < 0.05$), indicating some changes in conformation occur during the SPLITT fractionation. Despite the good agreement of actual PSDs with expected sizes and the noninvasive nature of the separation, it appears that the SPLITT has some effect on particle morphology and structure. Plots of shape factor against size (both longest and shortest dimension) indicated no significant variation with size in the <10-μm range (data not shown). However, at larger sizes, there is a qualitative indication that particles became less spherical, i.e., had lower shape factor values.

Fluorescence Analysis. Further analysis was performed on the bulk waters and on the SPLITT fractions by 3D EEM fluorescence and examples of these are shown in Figure 5. Although much work has been performed measuring fluorescence of HS and in natural waters, there is almost no published information on the variation of fluorescence with colloid or particle size in natural waters. Although qualitative, clear changes in the relative intensities of peaks T, A, and C are visible in the different size fractions. The >1-μm fraction has proportionately more fluorescence intensity at peak T. Further quantitative analysis was performed by correlating the intensities of peak T (tryptophan-like with excitation at both 220 and 280 nm), peak A and peak C (humic-like and fulvic-like, respectively) with both pH and particle size.

Peak T fluorescence intensity demonstrates no relationship with pH (excitation center at 220 nm, $r = 0.42$; 280-nm excitation center, $r = 0.11$), contrasting with strong pH dependency of peaks A and B (see next section) and suggesting that that the fluorophores responsible for peak T and peaks A and B are from different organic fractions. However, a strong, consistent dependency was found between the *a* and *b* size fractions from SPLITT (220-nm excitation center, 99% significance, *t*-test; 280-nm excitation center, 90% significance, *t*-test), indicating that up to 40% more tryptophan-like fluorescence was present in the >1-μm fraction.

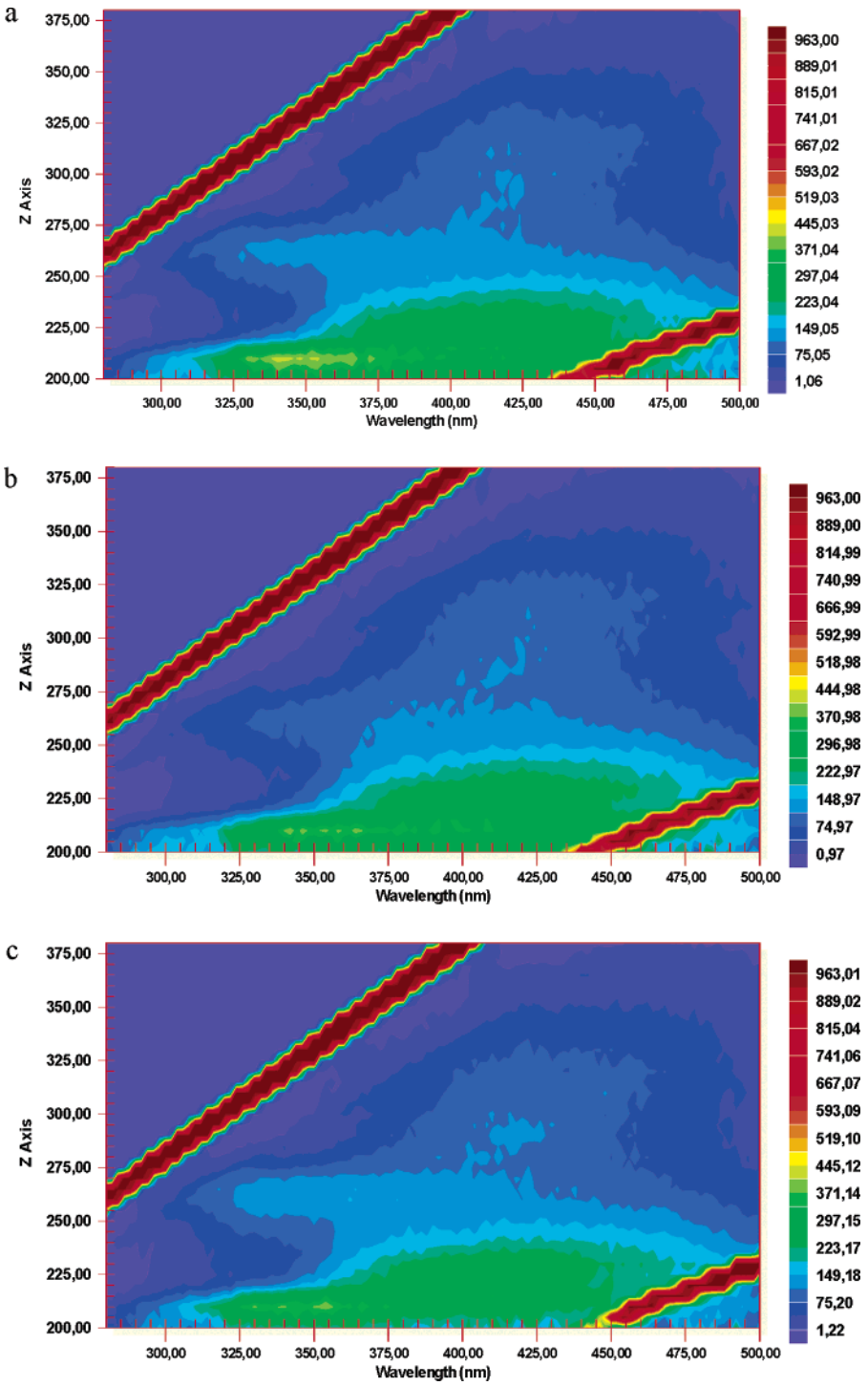

Figure 5. Three-dimensional EEM fluorescent matrixes showing response to unperturbed and size-fractionated lake water: (a) lake water; (b) <1-μm fraction; (c) >1-μm fraction.

The two fluorescent centers, represented by peaks A and C, have intensities that do not vary with SPLITT fraction but that are both significantly correlated with pH changes (peak A, $r = 0.73$, significant at 95% level; peak C, $r = -0.65$, significant at 90% level), as might be expected from the likely structural changes associated with HS on alteration of pH. Spectrophotometric properties of DOM are known to be highly sensitive to changes in solution pH.[19,31–33] However, the nonsignificant change of fluorescence with size indicates that these moieties are not free but associated quite strongly with other solid-phase material (clays, biological cells, etc.) present in natural waters. Extracted humic substances and their aggregates are usually between 1 and 100 nm[14] in size and if free would therefore only appear in the SPLITT a fraction (<1 μm). The ratio of fulvic-like to humic-like fluorescent

(31) Yang, A.; Sposito, G.; Lloyd, T. *Geoderma* **1994**, *62*, 327–344.

(32) Hautala, K.; Peuravuori, J.; Pihlaja, K. *Water Research*; Pergamon: New York, 2000; Vol. 34, pp 256–268.

(33) Patel-Sorrentino, N.; Mounier, S.; Benaim, J. Y. *Water Research*; Pergamon: New York, 2002; Vol. 36, pp 2571–2581.

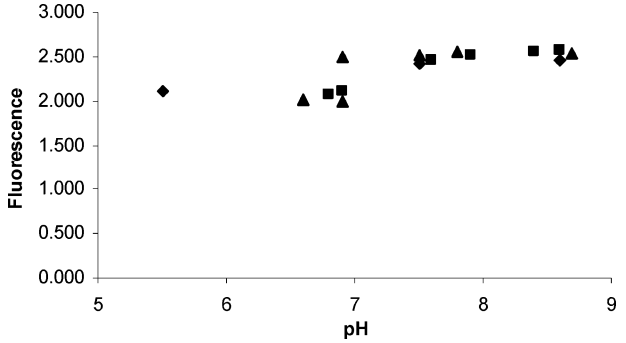

Figure 6. Variation of the humic-like (peak A) to fulvic-like (peak C) fluorescent intensity as a function of pH. Diamonds: unperturbed and perturbed waters. Squares: <1-μm fraction. Triangles: >1-μm fraction.

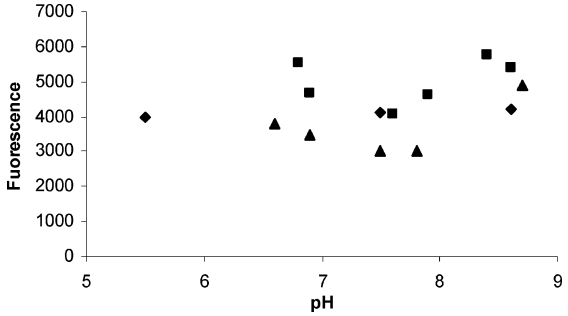

Figure 7. Variation of the fulvic-like (peak C) fluorescent intensity normalized to absorbance as a function of pH. Diamonds: unperturbed and perturbed waters. Squares: <1-μm fraction. Triangles: >1-μm fraction.

intensity is also, as previously observed,[33] correlated with pH (Figure 6), statistically so for the *a* fraction (95% confidence, $r = 0.95$). Peak A fluorescence, in comparison to peak C, exhibits a greater increase in intensity with increasing pH, suggesting differences in the ease of deprotonation of acidic/electron-donating functional groups between peaks A and C at different pH within the *a* fraction. Acid−base titration studies have seen similar differences in the acidities of fulvic and humic acids.[34] Finally, the ratio of fulvic fluorescence normalized to absorbance (Figure 7) varies as a function of size (*t*-test, 90% confidence) rather than pH (no statistical significance). Previous studies have suggested that this fluorescence efficiency is related to molecular size, which we demonstrate here using SPLITT.

CONCLUSION

The electron microscopy of bulk water and size fractions show that SPLITT provides an excellent, nonperturbing size fractionation, although careful validation by users needs to be performed on new and routine uses of SPLITT. Nevertheless, despite the absence of a membrane and expected minimal perturbation compared with filtration methodologies, morphological changes are apparent after SPLITT fractionation. Evidence is presented that tryptophan-like and humic- or fulvic-like fluorescence occurs primarily in different organic fractions. The traditional humic substances (HS)-type fluorescence is dependent on pH but not on size. However, fluorescence per unit absorbance is size dependent due to quenching reactions. The results suggest that the HS is chemically similar in both the colloidal and particulate fractions, most likely due to sorption onto larger material rather than aggregation of smaller HS units. The tryptophan-like fluorescence is primarily found in the particulate fraction, as expected given the likely microbial source of this fluorescence.

Received for review December 5, 2005. Accepted March 22, 2006.

AC0521347

(34) Lead, J. R.; Hamilton-Taylor, J.; Hesketh, N.; Jones, M. N.; Wilkinson, A. E.; Tipping, E. *Anal. Chim. Acta* **1994**, *294*, 319−327.